4-20-2005

Wave Field Migration as a Tool for Estimating Spatially Continuous Radar Velocity and Water Content in Glaciers

John H. Bradford
Boise State University

Joel T. Harper
University of Montana - Missoula

 DOI: 10.1029/2004GL021770

Wave field migration as a tool for estimating spatially continuous radar velocity and water content in glaciers

John H. Bradford
Center for Geophysical Investigation of the Shallow Subsurface, Boise State University, Boise, Idaho, USA

Joel T. Harper
Department of Geology, University of Montana, Missoula, Montana, USA

Received 15 October 2004; revised 17 January 2005; accepted 8 March 2005; published 20 April 2005.

[1] Normal-moveout velocity analysis can lead to significant overestimates of the velocity structure of temperate glaciers since most englacial reflectors approximate point scatters and violate the assumption of planar flat lying reflectors. Migration velocity analysis (MVA) is a tool that does not depend on the assumption of flat lying reflectors. MVA can provide laterally and vertically continuous velocity estimates from conventional common-offset radar sections. In a study of temperate Bench Glacier, Alaska, we used MVA coupled with dielectric modeling to estimate the distribution of water content along a cross-section of the glacier. We found the glacier has two layers, an upper layer with relatively low water content, and lower layer with relatively high water content. The ability to quantify hydrostratigraphy is important in understanding water storage and routing within glaciers. **Citation:** Bradford, J. H., and J. T. Harper (2005), Wave field migration as a tool for estimating spatially continuous radar velocity and water content in glaciers, *Geophys. Res. Lett.*, *32*, L08502, doi:10.1029/2004GL021770.

1. Introduction

[2] Electromagnetic (EM) wave propagation velocity is a material property that can be measured using ground penetrating radar (GPR). In glaciers, input of velocity structure to a dielectric mixing model can yield important details of the relative proportions of ice and water within the glacier body [*Macharet et al.*, 1993; *Murray et al.*, 2000]. Water within glaciers occupies three possible locations: within voids, within conduits, and within interstitial spaces and veins between ice grains [*Fountain and Walder*, 1998]. These features all play a role in water flux to the bed, through either routing or storage of surface melt. Since surface melt generation has been widely linked to the sliding activity of glaciers, understanding the spatial distribution of water within glaciers has important implications for glacier dynamics.

[3] Here we show that migration velocity analysis (MVA) of ground penetrating radar data may be used to determine the englacial water content of a temperate glacier. The method requires only constant offset radar data, and takes advantage of abundant radar scatterers common within temperate glacier ice. Through this analysis we found a study glacier to have a distinct two-layer hydrostratigraphy, giving us insight into the glacier's englacial hydrological processes.

0094-8276/05/2004GL021770$05.00

2. Migration Velocity Analysis

[4] The most common procedure for measuring radar velocity is the CMP method [*Yilmaz*, 2001] and it is commonly applied in the study of glaciers [*Blindow and Thyssen*, 1986; *Macharet et al.*, 1993; *Murray et al.*, 2000]. Key assumptions of the analysis are that velocity gradients are small, the maximum offset to depth ratio is small, and reflectors are flat lying and planar. Within the body of a temperate glacier, planar reflections are rarely observed while point scattering, typically from macro-scale water bodies, is common [*Bamber*, 1988; *Jacobel and Anderson*, 1987; *Watts and England*, 1976]. Due to the assumption of flat-lying reflectors, the apparent NMO velocity of the reflection for a point scatterer, measured from a CMP, is only correct when the CMP is directly over the scatterer [*Yilmaz*, 2001]. This problem is illustrated in Figure 1, which shows the specific case of a point scatterer embedded in a 0.168 m/ns medium at a depth of 100 m and maximum source receiver offset of 100 m. The velocity error grows rapidly with increasing horizontal CMP distance from the scatterer reaching an overestimate of nearly 40% when the CMP is 100 m from the scatterer. It is highly unlikely that sparsely located CMP gathers will be directly centered over the scattering hyperbolas. In most cases, englacial velocities will be overestimated.

[5] Alternatively, radar velocity can be measured directly from the scattering hyperbolas observed in common offset sections. In the study of a polythermal glacier, *Moore et al.* [1999] estimated englacial velocities by fitting the equation for a scattering hyperbola directly to travel times measured from common-offset GPR sections. While this method provides an accurate measure of velocity, it will not necessarily provide velocity estimates over the full glacier thickness since well defined point scatterers may not be present near the bed.

[6] Our approach utilizes wave field migration which is a data processing tool that seeks to place reflected energy at its point of origin; diffractions are collapsed and dipping reflections are moved to their correct spatial position. Thus, a correctly migrated reflection section is a spatially accurate image of subsurface electric permittivity contrasts [*Yilmaz*, 2001].

[7] Migration depends strongly on an accurate estimate of the GPR velocity distribution. When scattering events

and/or complexly dipping horizons (such as the glacier bed reflection) are present, it is possible to take advantage of this velocity dependence to measure the RMS velocity distribution using migration velocity analysis (MVA). With MVA, one first performs a series of constant velocity migrations with a range of velocities, then manually picks the velocity at a given depth/horizontal position that collapses diffractions and/or maximizes coherence along complexly dipping reflections. Thus, MVA can estimate the lateral and vertical RMS velocity distribution over the full thickness of a glacier. The interval velocity is then computed using Dix inversion [*Dix*, 1955].

[8] Although simple conceptually, MVA is not a "black-box" process and there are a number of potential problems and pitfalls including difficulty in identifying individual scattering events in a high density random reflectivity environment, out-of-plane reflections in 2D data, pegleg multiples, and precision limited by the distribution of scatterers. These problems must be evaluated on a case-by-case basis and steps should be taken to minimize artifacts. These steps may include analyzing the data in multiple pass bands, editing to avoid multiples, and smoothing the computed velocity models. We discuss methods for avoiding pitfalls at one site in the field example given below.

3. Estimating Water Content

[9] Given that radar velocity in water (~0.032 m/ns) is approximately one fifth that in ice (~0.168 m/ns) radar velocity can be a sensitive indicator of water content. To estimate water content from radar velocity, we use the Complex Refractive Index Method (CRIM) [*Greaves et al.*, 1996; *Huisman et al.*, 2003]. The CRIM equation is easily formulated for an arbitrary number of material components. In a three-phase system consisting of ice, water and air, we can arrange the CRIM equation to give water content as a function of bulk permittivity and porosity

$$\theta_W = \frac{\sqrt{K} - \sqrt{K_{ice}} - \phi\left(\sqrt{K_0} - \sqrt{K_{ice}}\right)}{\sqrt{K_W} - \sqrt{K_0}} \quad (1)$$

where θ_W is the water content by volume, ϕ is porosity. K_0, K_{ice}, and K_W are the relative permittivities of free space (1), dry solid ice (~3.2), and water (~86) respectively and are assumed constant. The effective permittivity K is related to the EM velocity by $\sqrt{K} = \frac{c}{v}$ where c is the speed of light in a vacuum, and v is the measured radar velocity. The three phase system is not well constrained - we must know either ϕ or θ_W to solve for the other - but in the two phase, water/ice system, $\phi = \theta_W$, and equation (1) is well constrained. Note that in the two phase case, the CRIM equation is comparable to the *Looyenga* [1965] and *Paren* [1970] relationships that are more commonly used in the study of glaciers [e.g., *Macharet et al.*, 1993; *Murray et al.*, 2000].

4. Field Example: Bench Glacier

[10] We acquired a series of GPR transects on the temperate Bench Glacier, Chugach Mountains, Alaska. The glacier occupies a relatively symmetrical trough with the ice thickness reaching 200 m near the glacier centerline.

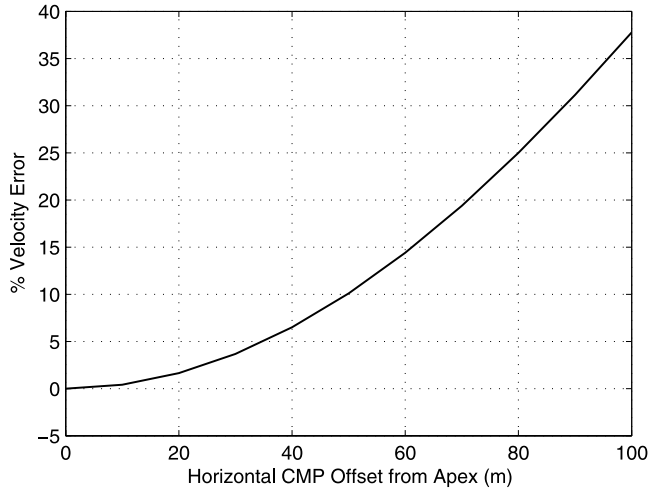

Figure 1. Velocity overestimate vs. horizontal CMP distance from a point scatterer using CMP NMO analysis. The medium velocity is 0.168 m/ns, depth to the scatterer is 100 m, and the source receiver offset range is 0–100 m.

Unique control for the radar experiments was offered by video imaging and water level data collected in 47 boreholes to the bed of the glacier [*Harper et al.*, 2005]. GPR data were collected on the ablation zone in early spring using a pulsed radar system with 25 Mhz antennas, 1 m trace spacing, and a 4 m transmitter/receiver offset. There was approximately 2 m of wet snow covering the glacier ice surface at the time of the survey. Video analysis indicated the ice body contained virtually no entrained sediment other than a few localities near the bed.

[11] Two distinct layers were imaged with the radar: a relatively transparent upper layer (Layer 1), and a lower layer (Layer 2) defined by numerous internal scatterers (Figures 2 and 3). The abrupt boundary between the two layers was 20–50 m below the glacier surface. Similar boundaries, corresponding to the cold/warm ice transition, are observed in polythermal glaciers [*Bamber*, 1987; *Jania et al.*, 1996; *Moore et al.*, 1999]. The coastal, low elevation glaciers of the Chugach Range, however, are temperate and the boundary is below the the winter cold wave.

[12] We computed the radar velocity distribution and volumetric water content along the profile using MVA and equation (1). Processing prior to MVA included a time-zero correction followed by a spherical spreading correction and an exponential gain correction. For MVA, we used constant velocity Stolt frequency/wavenumber (fk) migration [*Stolt*, 1978] at 0.005 m/ns intervals from 0.1 m/ns to 0.2 m/ns. We selected the 0.005 m/ns MVA interval as this was the velocity change with which we could confidently identify correct vs over or under migration, and therefore our velocity uncertainty is estimated at ±0.005 m/ns. To avoid multiples, we 1) only picked events that were not directly below shallower, high amplitude scatterers and 2) only picked events with the highest RMS velocity at any given time interval. This approach produced the smallest negative velocity gradient. Therefore, we reduce the chance of multiple induced artifacts, but minimize the potential to measure small scale velocity variations. Prior to computing the interval velocity distribution we applied a 50 m × 50 m

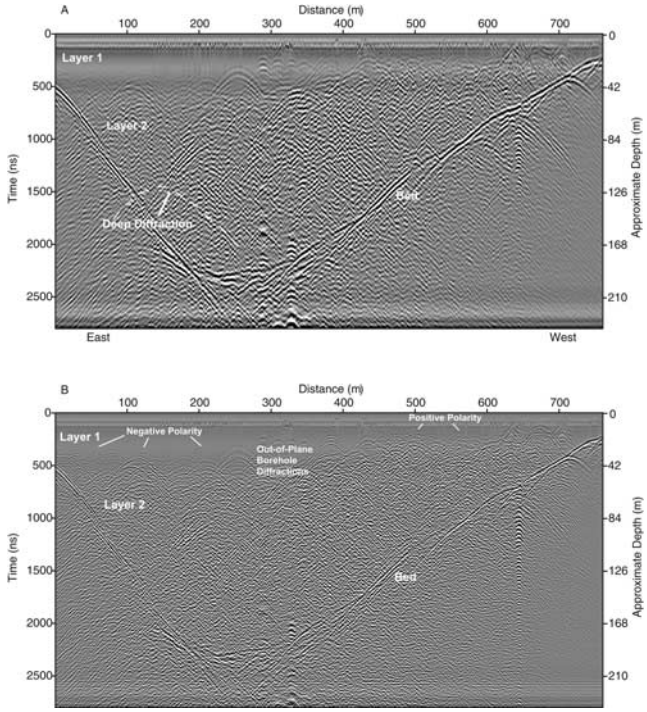

Figure 2. (a) 25 MHz GPR data with a 2–4–15–30 MHz bandpass filter applied. (b) same data as (a) with a 2–4–100–200 MHz bandpass filter. Layer 1 is characterized by a few scattering events, while Layer 2 is characterized by chaotic or random reflectivity. Although Layer 2 is difficult to interpret in both profiles, deep diffraction events can be isolated on the low pass filtered section. Reflections with opposite polarity are evident in Layer 1 suggesting that both water and air filled voids are present. Note that the depth scale is an approximation calculated using the average velocity.

2D smoother to the measured RMS velocity profile. Smoothing limits artifacts due to velocity picking errors. The size of the smoother was selected to ensure that two or more velocity picks were contained within every smoothing window. The smoothing operation was followed by Dix inversion [*Dix*, 1955]. We analyzed the data with both a narrow band, low-frequency filter (2–4–15–30 MHz, Figure 2a) to attenuate high frequency scatter thereby making it easier to isolate deep diffractions in Layer 2, and a broadband filter (2–4–100–200 MHz, Figure 2b) to preserve a high resolution image of the bed reflection and upper 50–80 m of the glacier. We made a total of 72 velocity picks, of these 37 were in Layer 1, 21 were in Layer 2, and 14 were located along the bed.

[13] The velocity in Layer 2 is substantially lower than that in Layer 1. Further, there is significant lateral and vertical velocity heterogeneity within each layer (Figure 3a). The velocity in Layer 1 generally decreases with depth, has an average velocity of 0.171 m/ns which is greater than the velocity of ice (0.168 m/ns), and has a maximum velocity of 0.181 m/ns. This result requires air filled void space in Layer 1. Conversely, Layer 2 has an average velocity of 0.152 m/ns and minimum velocity of 0.140 m/ns which are significantly slower than that of ice, suggesting that there is a significant increase in water content below the Layer 1/Layer 2 boundary. Assuming Layer 2 is fully water saturated, and using equation (1) (with $\phi = \theta_W$), we computed an average bulk porosity/water content in Layer 2 of 0.026 ± 0.008 and maximum bulk porosity of 0.05 ± 0.01. The uncertainty estimate is based on the range of values resulting from the velocity error of ±0.005 m/ns. We also computed the bulk porosity in Layer 1 assuming $\theta_W = 0$. This yielded an average porosity of 0.033 ± 0.008 and maximum porosity of 0.16 ± 0.008. Note that these values are likely low since there is actually some fractional saturation. Radar velocity depends primarily on the bulk properties of the system and it is not possible to differentiate between large or small scale void space so the porosity estimate includes bubbles, crevasses, cracks, conduits, veins etc.

[14] In the ice/water/air system there is an inherent ambiguity between porosity and water content. However, it is still possible to derive a reasonable estimate of the water content since the radar velocity depends strongly on bulk water content and weakly on unsaturated porosity [*Topp et al.*, 1980]. We assumed $\phi = 0.08$ given the likely porosity range of $\phi = 0.0 - 0.16$. At a velocity of 0.159 m/ns the solution to equation (1) with $\phi = 0.08$ is $\theta_W = 0.02$. This is within 0.008 of the solution for full water saturation ($\theta_W =$

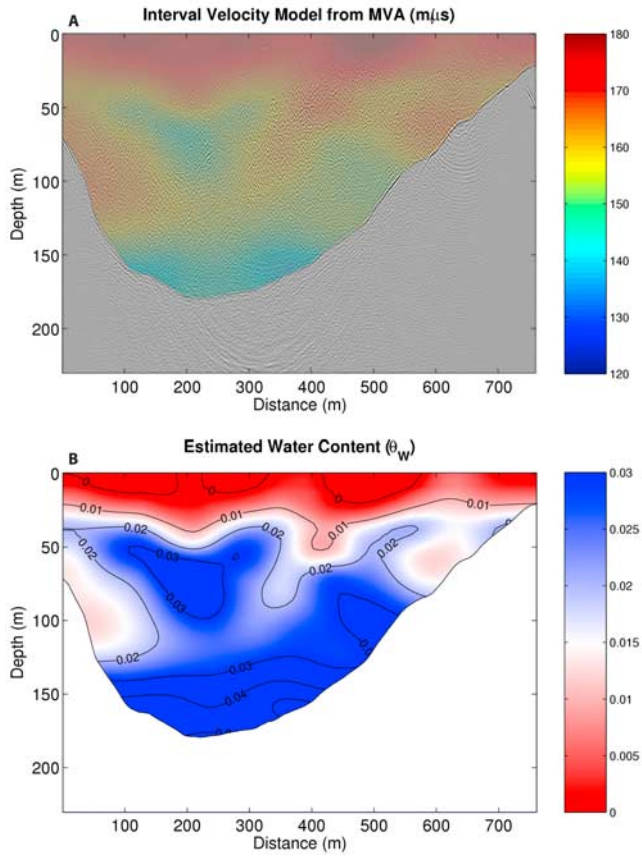

Figure 3. (a) Overlay of the interval velocity model across Bench Glacier derived from data shown in Figure 2 using MVA. Depth-converted migrated data are shown in the background. (b) Water content estimate using the CRIM equation with the velocity model in (a). There is a distinct increase in water content at the Layer 1/Layer 2 boundary. This boundary also correlates with the average piezometric surface measured in boreholes at the time of acquisition.

ϕ = 0.013). At lower velocities (higher water content) the solutions for the two cases vary by less than 0.008 for water contents up to 0.13. We conclude that the assumption of constant porosity results in minimal error in the resulting water content distribution and is likely lower than the uncertainty resulting from the velocity measurement or in the variation between different dielectric models.

[15] There is a significant increase in water content that correlates to the boundary between Layers 1 and 2. We interpret the boundary as defining a macroscale water table with low water content (0–0.02) in Layer 1 and relatively high water content (0.02–0.05) in Layer 2. *Blindow and Thyssen* [1986] credited a similar boundary between radar scattering/non-scattering layers in a temperate Austrian glacier to the "water table". Our interpretation is similar, only we further argue that the water table is present within macro scale voids (cf., grain scale pores and veins) that have some hydraulic connection to the bed. Our interpretation is based on, 1) numerous void spaces observed within this glacier via borehole video imaging, some of which are connected to the bed [*McGee et al.*, 2003], 2) the water level in two nearby boreholes correlate with the depth of the radar-boundary at the time of the radar surveys, and 3) individual scattering events with opposite polarity are present in layer 1 (Figure 2). The latter observation suggests the presence of both water filled and air filled voids in Layer 1, as the reflection coefficient between an ice/water interface is negative while that at an ice/air interface is positive.

[16] Analysis of ice cores from temperate glaciers have yielded water content values of up to 0.01 [*Raymond and Harrison*, 1975]. The ice core measurements sample the grain scale network of pores and veins, but not macro scale voids. Summing our borehole void space measurement with the published ice core measurements results in potential water content of 0.021 within Layer 2. This is within estimated uncertainty of the average value of 0.026 ± 0.008 we computed using MVA analysis and dielectric modeling. We present this latter comparison, not to suggest that all glaciers are the same, but merely to test our MVA results for reasonable agreement with other studies.

5. Conclusions

[17] MVA is a tool we can apply directly to conventional common-offset GPR data that does not depend on the assumption of flat lying, planar reflectors. Additionally, MVA allows us to simultaneously measure the moveout velocity of scattering diffractions while using coherence along complexly dipping reflections to guide our velocity picks. Because of this, the method has an inherent advantage over simply fitting the travel time curve of the scattering hyperbolas. On Bench Glacier, we used MVA coupled with dielectric modeling to estimate the water content distribution along a cross-section of the glacier. The reflectivity pattern, velocity model, and water content distribution indicates a two layer englacial hydraulic system. The upper layer has low water content, while the lower layer appears to have relatively high water content. In our interpretation, the boundary between the two layers defines a water table present in a macro-scale void system. This is consistent with nearby boreholes in which the average piezometric surface at the time of data acquisition correlates well with the layer boundary observed in the GPR data. This analysis shows a large amount of water is stored englacially – water that potentially plays a significant role in basal sliding dynamics.

[18] **Acknowledgment.** The National Science Foundation, Office of Polar Programs partially funded this work under Grant # OPP-0118488.

References

Bamber, J. L. (1987), Internal reflecting horizons in Spitsbergen glaciers, *Ann. Glaciol.*, *9*, 5–10.

Bamber, J. L. (1988), Enhanced radar scattering from water inclusions in ice, *J. Glaciol.*, *34*, 293–296.

Blindow, N., and F. Thyssen (1986), Ice thickness and inner structure of the Vernagtferner (Oetztal Alps): Results of electromagnetic reflection measurements, *Z. Gletscherkd. Glazialgeol.*, *22*, 43–60.

Dix, C. H. (1955), Seismic velocities from surface measurements, *Geophysics*, *34*, 180–195.

Fountain, A. G., and J. S. Walder (1998), Water flow through temperate glaciers, *Rev. Geophys.*, *36*, 299–328.

Greaves, R. J., D. P. Lesmes, J. M. Lee, and M. N. Toksoz (1996), Velocity variation and water content estimated from multi-offset, ground-penetrating radar, *Geophysics*, *61*, 683–695.

Harper, J. T., N. F. Humphrey, W. T. Pfeffer, T. Fudge, and S. O'Neel (2005), Seasonal evolution of subglacial water pressure, *Ann. Glaciol.*, in press.

Huisman, J. A., S. S. Hubbard, J. D. Redman, and A. P. Annan (2003), Measuring soil water content with ground-penetrating radar: A review, *Vadose Zone J.*, *2*, 476–491.

Jacobel, R. W., and S. K. Anderson (1987), Interpretation of radio-echo returns from internal water bodies in variegated glacier, Alaska, U.S.A., *J. Glaciol.*, *33*, 319–323.

Jania, J., D. Mochnacki, and B. Gadek (1996), The thermal structure of Hansbreen, a tidewater glacier in southern Spitsbergen, Svalbard, *Polar Res.*, *15*, 53–66.

Looyenga, D. E. (1965), Dielectric constants of heterogeneous mixtures, *Physica*, *31*, 401–410.

Macharet, Y. Y., M. Y. Moskalevsky, and E. V. Vasilensky (1993), Velocity of radio waves in glaciers as an indicator of their hydrothermal state, structure and regime, *J. Glaciol.*, *39*, 373–384.

McGee, B. W., J. T. Harper, N. F. Humphrey, and W. T. Pfeffer (2003), Water flow through widespread and interconnected void spaces at depth in a temperate glacier, *Eos Trans. AGU*, *84*(46), Fall Meet. Suppl., Abstract C11C-0850.

Moore, J. C., A. Palli, F. Ludwig, H. Blatter, J. Jania, B. Gadek, P. Glowacki, D. Mochnacki, and E. Isaksson (1999), High-resolution hydrothermal structure of Hansbreen, Spitsbergen, mapped by ground-penetrating radar, *Ann. Glaciol.*, *45*, 524–532.

Murray, T., S. W. Graham, M. Fry, N. H. Gamble, and M. D. Crabtree (2000), Englacial water distribution in a temperate glacier from surface and borehole radar velocity analysis, *J. Glaciol.*, *46*, 389–398.

Paren, J. G. (1970), Dielectric properties of ice, Ph.D. thesis, Univ. of Cambridge, Cambridge, UK.

Raymond, C. F., and W. D. Harrison (1975), Some observations on the behavior of liquid and gas phases in temperate glacier ice, *J. Glaciol.*, *14*, 213–233.

Stolt, R. H. (1978), Migration by Fourier transform, *Geophysics*, *43*, 23–48.

Topp, G. C., J. L. Davis, and A. P. Annan (1980), Electromagnetic determination of soil water content; measurements in coaxial transmission lines, *Water Resour. Res.*, *16*, 574–582.

Watts, R. D., and A. W. England (1976), Radio-echo sounding of temperate glaciers: Ice properties and sounder design criteria, *J. Glaciol.*, *17*, 39–48.

Yilmaz, O. (2001), *Seismic Data Analysis*, 2027 pp., Soc. of Explor. Geophys., Tulsa, Okla.

J. H. Bradford, CGISS MG-206, Boise State University, 1910 University Dr., Boise, ID 83725, USA. (johnb@cgiss.boisestate.edu)

J. T. Harper, Department of Geology, University of Montana, Missoula, MT 59812-1296, USA.